# ORR Activity and Stability of Co-N/C Catalysts Based on Silicon Carbide Derived Carbon and the Impact of Loading in Acidic Media

**P. Teppor,[1,*] R. Jager,[1] E. Hark,[2,**] I. Tallo,[1] U. Joost,[3] M. Kook,[3] P. Paiste,[4] K. Smits,[5] K. Kirsimae,[4] and E. Lust[1,**,z]**

[1] *Institute of Chemistry, University of Tartu, 50411 Tartu, Estonia*
[2] *Soft Matter and Functional Materials, Helmholtz Zentrum Berlin, 14109 Berlin, Germany*
[3] *Institute of Physics, University of Tartu, 50411 Tartu, Estonia*
[4] *Institute of Ecology and Earth Sciences, University of Tartu, 50411 Tartu, Estonia*
[5] *Institute of Solid State Physics, University of Latvia, 1063 Riga, Latvia*

A simple and facile synthesis method was used to produce two Co-N/C type oxygen reduction reaction (ORR) catalysts. The materials were initially characterized by utilizing a variety of physical methods. Most importantly, the XPS analysis revealed high amounts of pyridinic nitrogen and Co-$N_x$ species in the case of both studied Co-N/C catalysts. The electrochemical characterization showed that both of the synthesized Co-N/C catalysts have a high ORR activity in acidic media, displaying a half-wave potential of 0.70 V vs RHE. Additionally, the effect of varying the catalyst loading was studied and it was found that increasing the catalyst loading from 0.1 to 1.8 mg $cm^{-2}$ significantly improved the ORR activity and the electron transfer number. Finally, several catalysts were subjected to a week-long stability test in order to establish their activity degradation rates. It was found that increased degradation rates of the Co-N/C catalysts were established at decreased catalyst loadings.

A considerable amount of the high cost of a PEMFC stack can be attributed to the usage of platinum as a catalyst.[1,2] In addition to the already expensive price tag, the scarcity of platinum further impedes the large-scale commercialization of PEMFCs.

In order to overcome this obstacle, attention has been shifted toward developing more inexpensive and economically viable catalyst materials.[3–5] In this area, carbon materials doped with nitrogen and various transition metals (M-N/C, where M is usually Fe or Co) have shown promising results. Several factors have been shown to influence the final catalytic activity of these novel M-N/C catalysts. First, the best catalysts so far have been synthesized with either Fe or Co as the transition metal.[4–7] Concerning the choice of the nitrogen source, the selection is far more diverse. One possibility is to utilize a nitrogen-containing organic ligand which forms a stable complex with the metal cation. Highly active ORR catalysts have been synthe-sized using a wide array of ligands, for instance 2,2'-bipyridine,[8–10] 1,10-phenanthroline,[10,11] salen,[7] 2,4,6-tri(2-pyridyl)-s-triazine.[11] De-spite great advancements in improving M-N/C type catalysts, their ORR activity in acidic media is still inferior compared to commercial platinum catalysts.[5,12,13] Due to this considerable gap, more research is needed to further enhance these alternative catalyst materials.

Besides activity, another equally important aspect of any ORR catalyst is its stability, i.e., the ability to maintain activity toward the ORR after continuous utilization of the catalyst. Several authors have already presented data concerning the stability of their novel M-N/C catalysts in addition to their activity.[3,10,14] Based on these studies it is clear that the stability of these M-N/C type catalysts is severely lacking, especially when measured in acidic media. Accordingly, further research is needed to identify and synthesize catalysts with both high ORR activity and enhanced electrocatalytic stability.

An exceedingly important parameter that should be acknowledged is the loading of the catalyst. For platinum-based catalysts it has been found that varying the catalyst loading has a negligible effect on the ORR activity.[15,16] However, this is not the case when considering M-N/C type catalysts. Numerous studies have shown that altering the loading of an M-N/C catalyst has a serious effect on the electrochem-ical behavior, influencing both the half-wave potential and electron transfer number values.[9,13,17–20]

When looking at the catalytic activity of various materials it is important to consider whether the measurements were done in a solution or in fuel cell conditions.[13,20,21] A number of authors have demonstrated that transfering a catalyst material into a practical fuel cell causes the activity of the material to suffer.[12,22,23] The rational de-sign of cathode catalyst layers containing M-N/C type catalysts will become an increasingly more prominent issue in the near future.

Previously our workgroup used 5 different N precursors to synthesize Fe-N/C type ORR catalysts.[10] In that study, the most ac-tive catalyst materials were obtained with 2,2'-bipyridine and 1,10-phenanthroline and these compounds were selected as the N pre-cursors for the synthesis of our novel Co-N/C type catalysts. In our previous work we presented only first results about the activity and sta-bility of these Co-N/C materials in acidic media.[24] The present study provides a more detailed analysis of these materials. The catalysts are studied using a variety of physical characterization methods. Addi-tionally, one of the Co-N/C catalyst was chosen to investigate how the catalyst loading influences the ORR activity and the stability. A preliminary relation between the catalyst loading and electrochemical stability was established. Studying these Co-N/C catalyst materials in fuel cell conditions is the next necessary step in determining their true activity and the measurements are currently being prepared.

## Catalyst Synthesis

A carbon support material for synthesizing the following Co-N/C catalysts was made from silicon carbide (SiC, 98.5%, 320 grit powder, Alfa Aesar) by chlorinating ($Cl_2$, AGA, 99.99%, gas flow 100 ml $min^{-1}$) the powder at 1100° C and thereafter activating with $CO_2$ (AGA, 99.99%, gas flow 50 ml $min^{-1}$) for 3 hours.[25] This micro-mesoporous carbon was denoted as C.

A previously proven solution-based method was employed to synthesize the Co-N/C catalysts.[11,24,26] First, 46 mg of a cobalt com-plex compound (hexaamminecobalt(III) chloride, $[Co(NH_3)_6]Cl_3$, ≥99.0%, Fluka) was dissolved in Milli-Q+ water. Next, either 67 mg of 1,10-phenanthroline (≥99%, Aldrich) or 53 mg of 2,2'-bipyridine (ReagentPlus, ≥99%, Sigma-Aldrich) was also dissolved in Milli-Q+ water and the resulting nitrogen precursor containing so-lution was mixed together with the cobalt compound solution for 1 hour. Afterwards, 100 mg of the carbon powder was mixed into the previously prepared solution. After 2 hours of mixing with a magnetic stir bar and an ultrasonic bath, the solvent was removed with a ro-tary evaporator. Finally, the powder was heat-treated in argon (AGA,

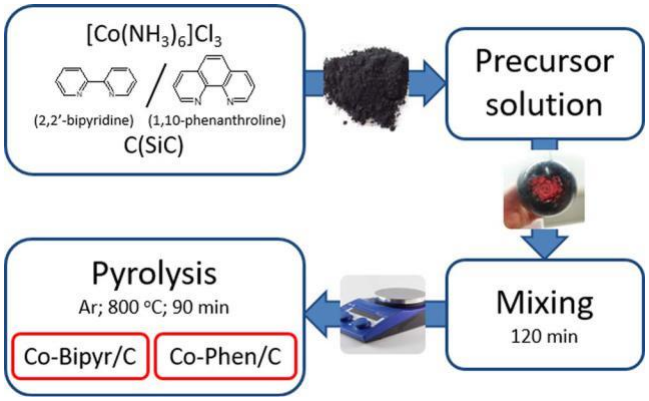


**Figure 1.** Outline of the synthesis of Co-N/C catalysts.

99.999%, gas flow 200 ml $min^{-1}$) at 800° C for 1.5 hours using a tube furnace. For both of the Co-N/C catalysts, the synthesis yield of the pyrolysis was nearly 70%. The synthesized catalysts were named in the text as Co-Phen/C and Co-Bipyr/C (Figure 1). A final catalyst ma-terial was synthesized using the previously described procedure but with the exclusion of the cobalt complex compound. 2,2'-bipyridine was selected as the nitrogen precursor and the resulting catalyst was named as Bipyr/C.

A commercial carbon catalyst containing 20 wt% of Pt (Pt-VulcanXC72, Fuel Cell Earth) was chosen as a reference material (named as Pt/V).

### Physical Characterization

The synthesized materials were analyzed using various physi-cal characterization methods. The transmission electron microscopy (TEM) images were obtained with a Tecnai G20 FEI instrument op-erating with 200 kV accelerating voltage in brightfield mode.

The X-ray photoelectron spectroscopy measurements were con-ducted using an electron energy analyzer (SCIENTA SES 100) equipped with a non-monochromatic twin anode X-ray tube (Thermo XR3E2) and Casa XPS software for data analysis.[27]

The amount of cobalt in the Co-N/C catalysts was acquired with an inductively coupled plasma mass spectrometer (ICP-MS, Agilent 8800) operated in the MS/MS mode and a helium (99.99%, the Linde Group, AGA) flow of 6 ml $min^{-1}$ in the collision cell. Prior to the mea-surements, the samples were dissolved in Aqua Regia (3:1 HCl:$HNO_3$, CarlRoth ROTIPURAN Supra acids) at 100° C for 24 h under reflux conditions and centrifuged at 4000 rpm for 20 min.

The catalyst materials were studied with the low-temperature ni-trogen sorption method using an ASAP 2020 system (Micromeritics). The obtained data was subjected to a 2D non-local density functional theory based model for carbons with heterogeneous surfaces to attain the pore size distribution. The surface area of the catalyst powders was evaluated with the Brunauer-Emmett-Teller (BET) multipoint theory applied to the relative pressure range from 0.05 to 0.2.[28]

The thermogravimetric analysis (TGA) was conducted with an STA 449 F3 Jupiter device. A small amount (~10 mg) of catalyst powder was placed on an alumina crucible, which was raised to and held at 30° C until the sample mass was stabilized. The thermogravi-metric curves were registered from 30 to 900° C at a heating rate of 10° C $min^{-1}$ under a nitrogen flow of 60 ml $min^{-1}$.

### Electrochemical Characterization

The catalyst ink was prepared by mixing the synthesized cata-lyst powder (C, Co-Phen/C, Co-Bipyr/C, Bipyr/C or Pt/V) with iso-propanol (99.0%, Sigma-Aldrich), Milli-$Q^+$ water and a Nafion 117 solution (~5%, Sigma-Aldrich, Aldrich Chemistry). The amounts of the added liquids were varied to achieve final catalyst loadings of 0.8 ± 0.1 mg $cm^{-2}$ for all catalysts studied. The resulting catalyst mixture was then treated in an ultrasonic bath for 1 hour. Finally, the catalyst ink was deposited onto polished glassy carbon disk electrodes and left to dry overnight.

Three additional catalyst inks were prepared from both Co-Phen/C and Co-Bipyr/C to study the effect of the material loading on the ORR catalytic behavior. To achieve this, Co-Phen/C or Co-Bipyr/C powders were mixed with the previously mentioned liquids, but the added amounts were chosen so that the final catalyst loadings were 0.1 ± 0.05, 0.4 ± 0.1, and 1.8 ± 0.1 mg $cm^{-2}$.

The electrochemical characterization of the catalyst materials was conducted using a three-electrode setup in a glass electrochemical cell. Before the experiments, all used equipment was washed with concentrated $H_2SO_4$ (95.0-97.0%, Sigma-Aldrich) and rinsed with Milli-$Q^+$ water to ensure a minimal amount of contaminants. The measurements were conducted in a 0.1 M $HClO_4$ solution (67–72% $HClO_4$, Sigma-Aldrich, Fluka Analytical). A saturated calomel elec-trode (SCE, REF421, Radiometer analytical) and a glassy carbon rod were used as the reference and as the counter electrode, respectively. The potential values were converted to the RHE scale (the potential of SCE versus RHE was determined to be 317 mV). The catalyst materials were studied using the rotating disk electrode (RDE) and cyclic voltammetry (CV) methods. In the case of RDE the scan rate was fixed at 10 mV $s^{-1}$ and the rotation speed was varied from 500 to 3000 rpm. For CV measurements the scan rate was varied from 5 to 200 mV $s^{-1}$. Additionally, the measured current values have been corrected against ohmic potential drop (iR-drop) using the resistance value of 21 ± 1 determined with electrochemical impedance spec-troscopy. Four different electrodes with the same composition were prepared and measured to confirm the reproducibility of the obtained data.

### Results and Discussion

***TEM.***—The TEM images were used to visualize the structure of the carbon support (C) and to study the effects of adding cobalt and nitrogen. It can be seen that the unmodified carbon has both graphitic and amorphous areas (Figure 2a). Additional TEM images taken for the synthesized Co-N/C catalysts (Figures 2b and 2c) show layers of amorphous carbon surrounding cobalt nanoparticles, as previously shown in our study.[24] A similar structure was reported in a work discussing analogous Fe-N/C catalysts.[26] In that work, however, the Fe particles were covered by well-organized graphitic carbon layers, whereas the Co-N/C catalysts discussed presently contain predom-inantly amorphous carbon layers. Roughly 100 nanoparticles were measured to analyze the average cobalt particle size of the Co-N/C catalyst. According to the particle size distribution (Figure 2d) most of the particles for Co-Phen/C are in the range from 20 to 40 nm, whereas for Co-Bipyr/C the distribution is spread out and the parti-cles are overall larger in size (from 30 to 60 nm). Particles of such size have been observed for other Co-N/C catalyst materials prepared by utilizing similar synthesis methods.[29–31] Zhou et al.[31] showed that the size of the Co nanoparticles increases with increasing pyrolysis temperature.

***XPS.***—The synthesized Co-N/C and Bipyr/C materials were sub-jected to a thorough XPS analysis to study their chemical and elemen-tal composition (Table I and Figure 3). Figures 3a and 3b show the complete and detailed Co2p (inset) regions measured for Co-Phen/C and Co-Bipyr/C, respectively. The Co2p peak at around 780 eV ex-hibits an extremely low intensity peak, which can be deconvoluted into three separate peaks. The broad peak at 787 eV is a measurement satel-lite characteristic to $Co_3O_4$.[32] Two different oxidation states of cobalt can be found at 780 eV and 782 eV. The peak at 780 eV can be assigned to various cobalt oxides or cobalt carbide, which all display similar binding energies.[33] The second peak has a binding energy almost identical to the reported binding energy of Co-$N_4$ moieties.[33] Metallic cobalt was not detected in neither of the studied materials, which can be explained by the high surface sensitivity of the method and cobalt

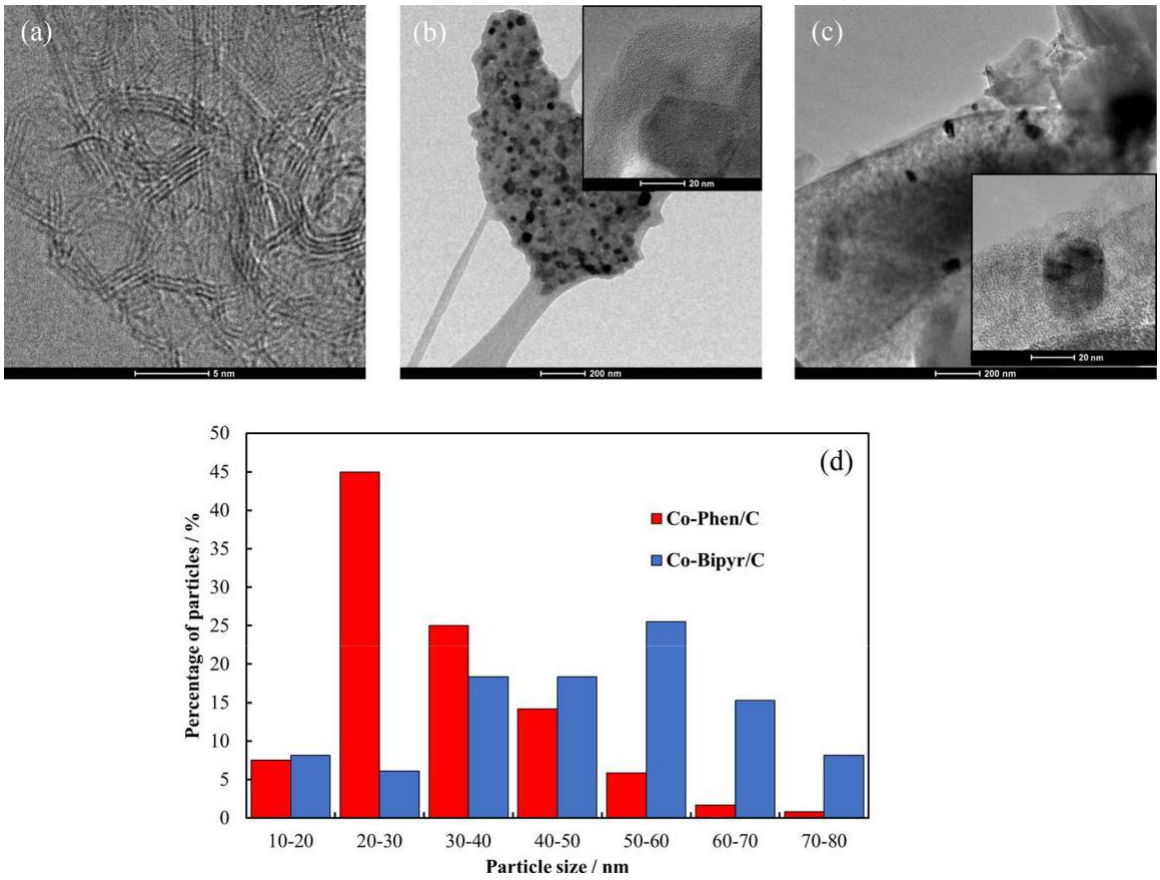


**Figure 2.** TEM images for materials: (a) C, (b) Co-Phen/C, and (c) Co-Bipyr/C. (d) Particle size distribution for Co-N/C catalysts (noted in Figure).

**Table I. XPS data for Co-N/C catalysts.**

| | | | | | Form of nitrogen (%) | | | | |
|---|---|---|---|---|---|---|---|---|---|
| Material | C (at%) | Co (at%) | O (at%) | N (at%) | Pyridinic | Co-$N_x$/ Amine | Pyrrolic | Quaternary | N-O species |
| Co-Bipyr/C | 94 | 0.5 | 5.5 | 1.4 | 36 | 26 | 27 | 6 | 6 |
| Co-Phen/C | 94 | 0.9 | 3.0 | 2.2 | 35 | 31 | 22 | 8 | 4 |
| Bipyr/C | 96 | - | 2.9 | 1.6 | 5 | 18 | 31 | 43 | 3 |

nanoparticles being covered with layers of carbon as illustrated by the TEM images. The N1s (Figure 3d) region measured at around 400 eV for the Bipyr/C and Co-N/C catalysts yields five distinctive nitrogen electronic states widely analyzed in previous works:[11,33−36] pyridinic N at 397.9 eV, Co-$N_x$/amine N at 399.1 eV, pyrrolic N at 400.7 eV, quaternary/graphitic N at 402.6 eV, and N-O species at 404.7 eV. Most of the nitrogen found in both Co-N/C samples is in the pyridinic and Co-$N_x$ forms (Table I and Figure 3d inset), which have been proposed as the main components of the active sites for the ORR.[11,34−37] The Bipyr/C sample, however, contains only a minimal amount of pyri-dinic N and consists mostly of quaternary/graphitic N (Table I and Figure 3d inset).

***ICP-MS.***—ICP-MS was used to quantitatively determine the amount of cobalt in the synthesized materials. The measurements show that 5.8 wt% of cobalt for Co-Bipyr/C and 3.7 wt% for Co-Phen/C remained in the finished catalysts. After converting these val-ues to at%, the results were 1.2 at% and 0.8 at% for Co-Bipyr/C and Co-Phen/C, respectively. In the case of Co-Bipyr/C, ICP-MS showed an almost two times larger amount of cobalt compared to XPS (Table I), which can be explained by the encapsulation of the cobalt nanoparticles. For Co-Phen/C, the cobalt amount values obtained by ICP-MS and XPS are equal when considering the margin of measure-ment errors.

***$N_2$ sorption analysis.***—The highly porous catalyst materials were further characterized using the widely spread nitrogen adsorption analysis method. A brief analysis of C, Co-Bipyr/C, and Co-Phen/C has been presented in our previous work.[24] The BET surface area ($S_{BET}$), micropore surface area ($S_{micro}$), micropore volume ($V_{micro}$), and total pore volume ($V_{tot}$) values are reported in Table II. $V_{tot}$ was calculated at a relative pressure of 0.95 and $V_{micro}$ was obtained using the t-plot method supplemented with the Harkins and Jura thickness values for the porous adsorption carbon layer between 5 and 90 Å.[38] The un-modified carbon has a large surface area and is mostly microporous. Bipyr/C displays almost identical surface area and pore volume values compared to the unmodified carbon. Modifying the carbon with both a nitrogen-containing ligand and a cobalt complex compound notice-ably decreases the surface area and pore volume. For Co-Phen/C the surface area and pore volume decrease is more prominent. Plotting out the pore size distribution reveals that almost all of the pores are around 1–2 nm in size for all of the studied materials. In a recent article, Ban-ham et al.[13] demonstrated that extremely high current densities are attainable with catalysts consisting primarily of pores <3 nm in di-ameter. It can be argued that during the catalyst synthesis the cobalt

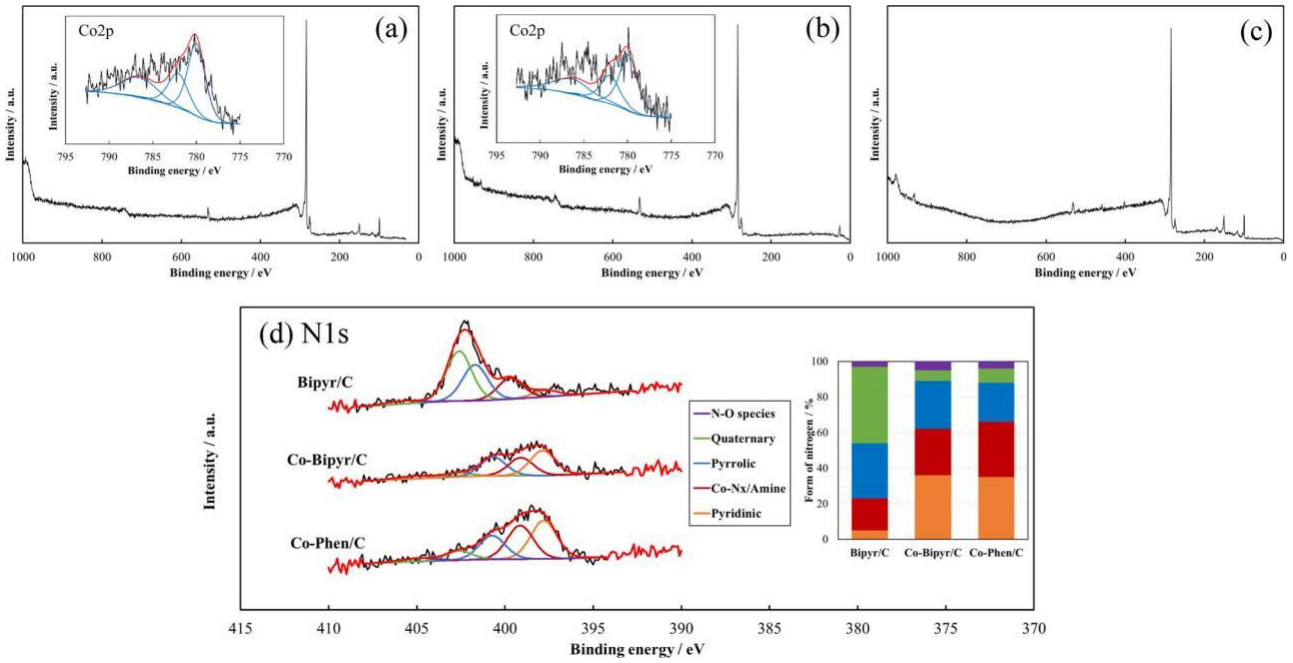


**Figure 3.** The wide scan and detailed Co2p (insets) XPS spectra for (a) Co-Phen/C and (b) Co-Bipyr/C, and wide scan XPS spectrum for Bipyr/C (c). The detailed N1s spectra (d) and the proportion of nitrogen species (inset) for synthesized catalysts (noted in Figure).

**Table II. $N_2$ sorption analysis data.**

| Material | $S_{BET}$ / $m^2 \cdot g^{-1}$ | $S_{micro}$ / $m^2 \cdot g^{-1}$ | $V_{micro}$ / $cm^3 \cdot g^{-1}$ | $V_{tot}$ / $cm^3 \cdot g^{-1}$ |
|---|---|---|---|---|
| C | 1639 | 1575 | 0.72 | 0.83 |
| Bipyr/C | 1579 | 1439 | 0.70 | 0.80 |
| Co-Bipyr/C | 988 | 960 | 0.44 | 0.49 |
| Co-Phen/C | 641 | 634 | 0.29 | 0.32 |

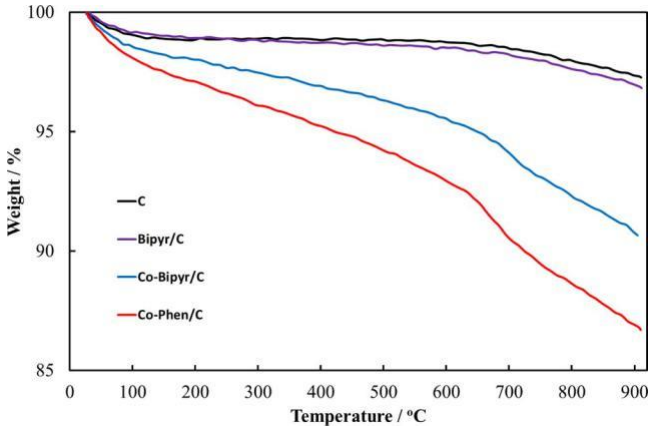


**Figure 4.** TGA curves measured for the studied materials (noted in Figure).

and nitrogen complex compounds adsorb equally in pores of different sizes and no significant micropore blockage occurs.

***TGA.***—Thermogravimetric analysis was conducted to study the thermal stability of the catalyst materials (Figure 4). A significant initial weight loss at the start of the measurements can be attributed to water evaporation. Between 100 to 700° C both the unmodified carbon and Bipyr/C are thermally stable. For these materials, a slightly larger weight loss can be noticed starting from around 700° C, which can be related to the desorption of various surface functional groups as CO and $CO_2$.[39] The TGA curve for Bipyr/C catalyst is comparable with C rather than with Co-Bipyr/C indicating that the doping of the carbide derived carbon with Bipyr precursor has not changed the microstructure of the carbon (Table II) confirmed by the low temperature $N_2$ sorption method.

The Co-Bipyr/C catalyst displays a more notable weight loss than Bipyr/C, which indicates a higher concentration of more volatile sur-face compounds due to differences in the surface chemistry of the catalysts demontrated by XPS (Table I). Additionally, the form of the nitrogen contributing with or without metal content influences the ther-mal decomposition of the catalyst. A sharper decrease in weight can be seen at around 650° C and 700° C for Co-Phen/C and Co-Bipyr/C, respectively. Overall, Co-Bipyr/C displayed a higher residual mass than Co-Phen/C.

***Electrochemical results.***—The background current corrected ORR curves measured in 0.1 M $HClO_4$ solution at 3000 rpm for various systems are presented in Figure 5. The material synthesized by adding only the nitrogen precursor to the carbon support, Bipyr/C, had a nearly identical oxygen reduction behavior ($E_{1/2}$ = 0.25 V vs RHE) compared to the base carbon ($E_{1/2}$ = 0.24 V vs RHE). De-spite the fact that Bipyr/C contains a considerable amount of nitrogen (Table I), most of it is in the quaternary/graphitic form.[36] This means that the procedure used in this work cannot be used to produce ac-tive N-C type catalysts. However, when modifying the carbon support with both nitrogen and cobalt the ORR activity increases remarkably ($E_{1/2}$ = 0.70 V vs RHE for both Co-N/C catalysts). The electron trans-fer number ($n_L$) values (Table III) have been calculated according to the Levich equation and using the parameters presented in our previ-ous work.[24] The resulting $n_L$ values were found to be 2.1 ± 0.1 for the less active catalysts (C and Bipyr/C) and ~2.7 for the Co-N/C cata-lysts. As already discussed in our previous work as well as by other

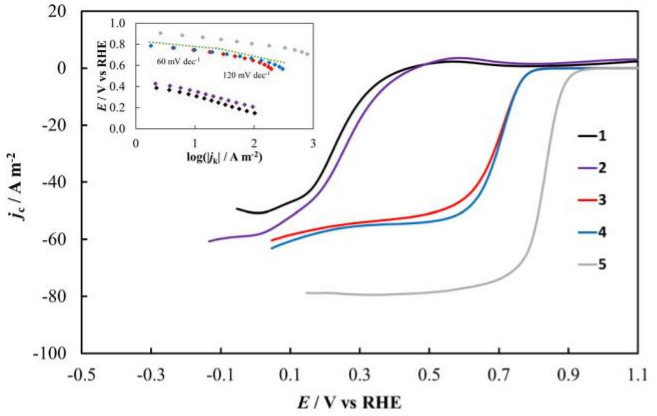


**Figure 5.** Background current corrected ORR curves measured in 0.1 M $HClO_4$ solution at 3000 rpm and scan rate 10 mV $s^{-1}$ for the studied catalyst materials: C (1), Bipyr/C (2), Co-Phen/C (3), Co-Bipyr/C (4), and Pt/V (5). Inset- corresponding Tafel plots.

**Table III. Half-wave potential and electron transfer number values for the studied catalyst materials.**

| Material | $E_{1/2}$ (V vs RHE) | $n_L$ (calculated at $E$ = 0.17 V vs RHE) |
|---|---|---|
| C | 0.24 ± 0.01 | 2.1 ± 0.1 |
| Bipyr/C | 0.25 ± 0.01 | 2.1 ± 0.1 |
| Co-Bipyr/C | 0.70 ± 0.01 | 2.7 ± 0.1 |
| Co-Phen/C | 0.70 ± 0.01 | 2.6 ± 0.1 |
| Pt/V | 0.83 ± 0.01 | 3.8 ± 0.1 |

authors,[4,24,40–42] this means the addition of both a transition metal and nitrogen creates new active sites which promote either the direct re-duction of oxygen to water or the 2 + 2-electron pathway. Despite the large increase in activity, the synthesized Co-N/C catalysts are still notably less active than the commercial Pt/V catalyst which displays a half-wave potential of 0.83 V vs RHE and a high electron transfer number of 3.8 ± 0.1.

The considerable oxygen reduction activity of the synthesized Co-N/C catalysts can be related to the similar nitrogen composition of both catalysts (Table I and Figure 3d inset). More specifically, both Co-Bipyr/C and Co-Phen/C have high amounts of pyridinic nitrogen and Co-$N_x$ species, which have frequently been tied to high ORR activity.[9,11,34–37] In contrast, the metal-free Bipyr/C contains only a small amount of pyridinic nitrogen. This significant disparity sug-gests that the active sites in the catalysts under study are related to either pyridinic nitrogen or Co-$N_x$ species.

Using the Koutecky-Levich analysis data, the Tafel plots were constructed for all studied catalysts (Figure 5 inset). For both Co-N/C catalysts it is possible to divide the plots between two linear regions with two different slope values, ~60 mV $dec^{-1}$ in the low current density region and ~120 mV $dec^{-1}$ in the high current density region. This result suggests that the mechanism of the ORR changes depending on the applied voltage. It has been proposed that in the case of 60 mV $dec^{-1}$ oxygen adsorption can be simulated using the Temkin isotherm and for 120 mV $dec^{-1}$ by the Langmuir isotherm.[43] The Tafel plot values obtained for unmodified C and Bipyr/C are significantly higher (~145 mV $dec^{-1}$), indicating considerably more sluggish ORR kinetics.[44]

***Catalyst loading studies.***—To gain insight into how the catalyst loading affects the oxygen reduction behavior, electrodes with vari-ous loadings of Co-Phen/C and Co-Bipyr/C were prepared and studied using the CV and RDE method. Figure 6a shows the oxygen reduc-tion CV curves measured for both catalysts at loadings ranging from 0.1 ± 0.05 to 1.8 ± 0.1 mg $cm^{-2}$. Increasing the catalyst loading

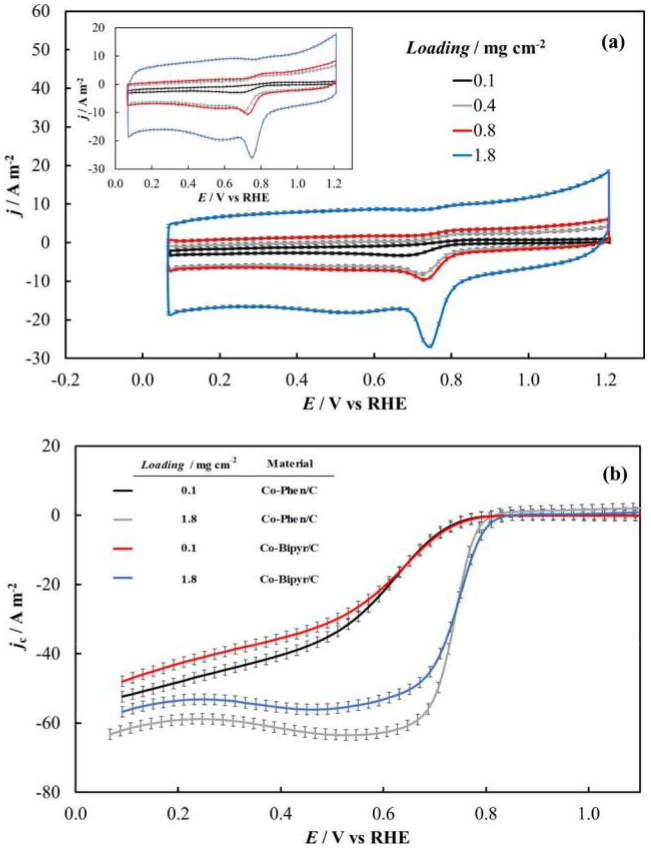


**Figure 6.** CV curves for (a) Co-Phen/C and (inset) Co-Bipyr/C catalysts with various catalyst loadings (noted in Figure) measured at scan rate 5 mV $s^{-1}$. (b) Background current corrected RDE data for Co-N/C catalysts with various catalyst loadings (noted in Figure) at 3000 rpm and scan rate 10 mV $s^{-1}$. Measured in 0.1 M $HClO_4$ solution.

significantly increases the intensity of the oxygen reduction peak and slightly shifts the peak toward more positive potential values. Addi-tionally, the capacity of the catalyst increases with electrode loading indicating that the loading has a considerable effect on the capacitive behavior of the catalyst.

The RDE measurements confirm the results obtained using CV and it can be seen that the oxygen reduction activity of the mate-rial strongly depends on the catalyst loading (Figure 6b). Electrodes with the lowest loading (0.1 ± 0.05 mg $cm^{-2}$) display substantially smaller currents than electrodes with higher loadings in both the mixed-kinetics and mass transfer limited regions. It is interesting to mention that for the catalyst with the loading of 0.1 ± 0.05 mg $cm^{-2}$ the diffusion limited current region has not properly developed into a plateau. As the catalyst loading is increased, the electrode half-wave potential shifts toward more positive values. This occurrence can be explained by the larger amount of active sites which in turn decreases the overpotential.[13]

Calculating the value of $n_L$ (corresponding to the different catalyst loadings) reveals that varying the loading has a significant effect on the outcome. The catalysts with larger loadings (1.8 ± 0.1, 0.8 ± 0.1, and 0.4 ± 0.1 mg $cm^{-2}$) all exhibit similar $n_L$ values of 2.6 ± 0.2. However, decreasing the catalyst loading down to 0.1 ± 0.05 mg $cm^{-2}$ reduces the electron transfer number to 2.0 ± 0.1, which is comparable to the unmodified carbon. This occurrence can be explained by the highly porous structure of the studied catalysts. A larger catalyst loading means the produced hydrogen peroxide molecules have to travel a longer distance before exiting the porous structure, thus having a higher chance of interacting with another active site and reducing further, as clearly demonstrated by Bonakdarpour et al.[17]

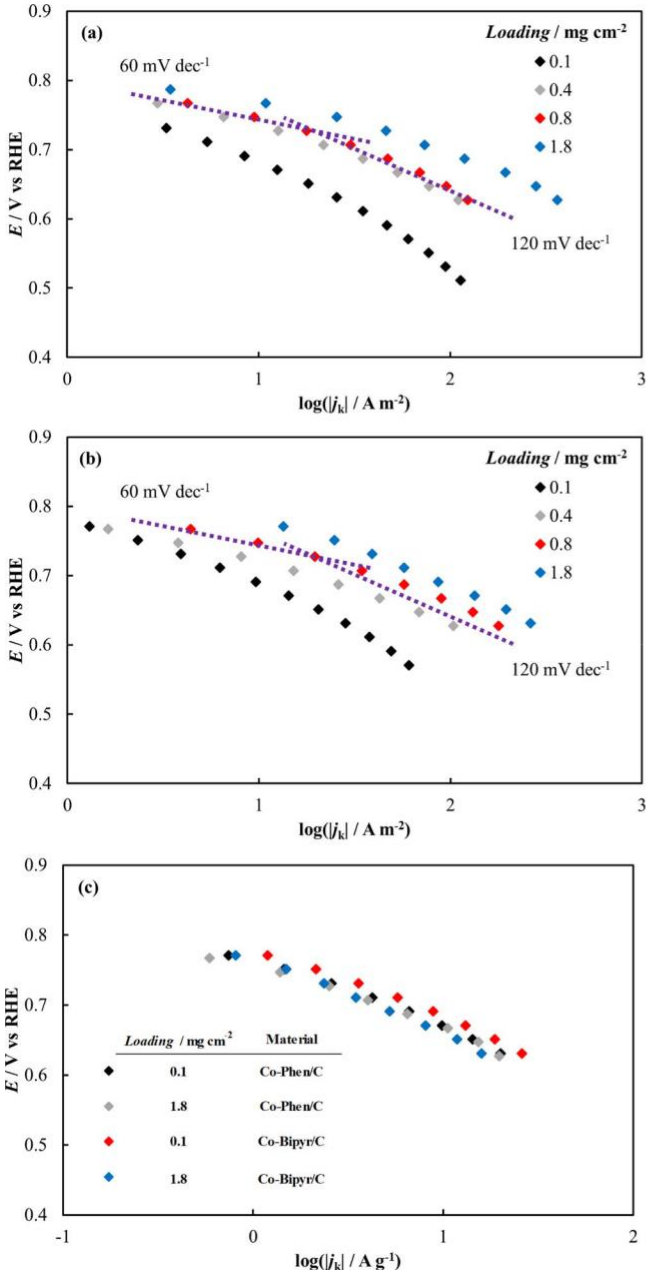


**Figure 7.** Tafel plots calculated from RDE data for the catalysts (a) Co-Phen/C and (b) Co-Bipyr/C at various loadings (noted in Figure) when considering current densities. The 60 mV dec$^{-1}$ and 120 mV dec$^{-1}$ lines correspond to the theoretical slope values. (c) Tafel plots calculated from RDE data for Co-N/C catalysts at various loadings when considering specific currents.

Using the Koutecky-Levich analysis, Tafel plots were constructed for all studied catalyst loadings (Figures 7a and 7b). Constructing the Tafel plots while considering the specific currents (A g$^{-1}$) instead of current densities (A m$^{-2}$) reveals that the resulting Tafel plots overlap (Figure 7c). This could indicate that the inherent reaction mechanism for the studied catalyst material does not depend on the loading.

The Co-N/C catalysts synthesized in the present work were compared to similar catalysts synthesized with iron (Fe-Phen/C and Fe-Bipyr/C). When using cobalt instead of iron as the transition metal, the half-wave potential value of the catalyst can be improved by 40 mV.[10] From this result, it can be argued that the choice of the used transition metal (either Co or Fe) during the synthesis affects the final catalytic activity.[7]

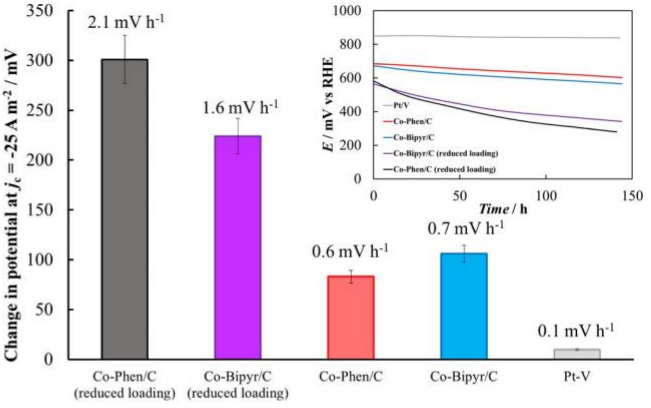


**Figure 8.** Change in potential at $j_C = -25$ A m$^{-2}$ after the stability mea-surements for various catalyst materials (noted in Figure) and inset- electrode potential at a fixed current density (−25 A m$^{-2}$) measured at 24 h intervals.

***Stability tests of the catalysts.***—The electrochemical stability tests with a duration of 140 hours were carried out using the same method described previously by our workgroup.[10,24,26] The voltammograms at rotation rates of 1000, 2000 and 3000 rpm were measured at roughly 24 h intervals. Between the activity measurements the catalysts were constantly cycled in an argon environment at 1 mV s$^{-1}$ from 0.21 to 1.23 V vs RHE.

The catalysts Co-Bipyr/C and Co-Phen/C with similar loadings of 0.4 ± 0.1 mg cm$^{-2}$ were subjected to the stability test. In our previous work we established that both of the studied Co-N/C catalysts exhibit decreased current density values in both the mixed kinetics and diffusion-limited regions as a result of the stability measurements.[24]

The beginning-of-test and end-of-test performances of the cata-lysts at $j_C = -25$ A m$^{-2}$ were assessed and the change in potential is presented in Figure 8, while Figure 8 inset shows the electrode potential measured at roughly 24 h intervals. A considerable perfor-mance decline was noted in the case of both catalysts. The calculated potential difference values correspond to electrode potential decrease speed values of 0.7 and 0.6 mV h$^{-1}$ for Co-Bipyr/C and Co-Phen/C, respectively. Thus, both of the synthesized Co-N/C catalysts display comparable degradation rates, which can possibly be attributed to their similar chemical composition as determined by XPS.

For comparison the stability of the Pt-V catalyst was assesed under similar conditions. The results of the measurements (Figure 8) indicate that the electrode potential of the commercial Pt/V catalyst decreased by only 10 mV, which corresponds to a degradation rate of 0.1 mV h$^{-1}$.

Additional stability tests were conducted with reduced loadings (0.1 ± 0.05 mg cm$^{-2}$) of Co-Phen/C and Co-Bipyr/C. At $j_C = -25$ A m$^{-2}$ the calculated performance declines were 2.1 mV h$^{-1}$ and 1.6 mV h$^{-1}$ for Co-Phen/C and Co-Bipyr/C, respectively. A first comparison reveals that differences in Co average particle size observed by TEM (Figure 2d) seem to influence the stability at reduced loading. The experimental data revealed that the catalysts with reduced loadings suffered from significantly larger decreases in activity than the catalysts with larger electrode loadings (Figure 8) indicating that the stability of a catalyst strongly depends on the loading. This means an increased loading significantly contributes toward a material be-ing more stable in regard to oxygen reduction, possibly due to the considerably smaller amount of produced $H_2O_2$.[45]

## Conclusions

In this work we presented physical and electrochemical characterization results of our novel Co-N/C type catalysts based on activated silicon carbide derived carbon. The catalyst materials were synthe-sized using a simple and robust one-pot synthesis method. The phys-ical characterization revealed that both of the Co-N/C catalysts had

similar nitrogen compositions and were mostly comprised of micropores. The validity of the chosen synthesis method was confirmed by the electrochemical measurements in acidic media, which revealed that co-doping the carbon support with Co and N increased the half-wave potential from 0.24 V up to 0.70 V vs RHE. Compared to a similar Fe-Phen/C catalyst synthesized in our previous work, the Co-Phen/C catalyst presented in this work is more active toward the ORR with a 40 mV more positive half-wave potential value. Varying the loading of the Co-Phen/C and Co-Bipyr/C catalysts had a significant impact on the electrochemical activity. It was shown that reducing the catalyst loading down to 0.1 ± 0.05 mg $cm^{-2}$ lowered the electron transfer number from 2.6 to 2.0, possibly due to the decreased likelihood of $H_2O_2$ reducing further in another active site.

Both Co-N/C catalysts were subjected to a stability test, which revealed that as a result of 140 hours of potential cycling, these materials exhibited similar degradation rates of 0.6 mV $h^{-1}$ and 0.7 mV $h^{-1}$ for Co-Phen/C and Co-Bipyr/C, respectively. More im-portantly, it was shown that Co-Phen/C and Co-Bipyr/C with reduced loadings (0.1 ± 0.05 mg $cm^{-2}$) displayed larger performance declines of 2.1 mV $h^{-1}$ and 1.6 mV $h^{-1}$, respectively. These results suggest that reducing the catalyst loading has a negative impact on both the stability and activity of the catalysts under study.

Determining whether the synthesized Co-N/C catalysts retain their activity in fuel cell conditions is the next necessary step and the measurements are in progress.

## Acknowledgments

This work was supported by the EU through the European Regional Development Fund under projects TK141 “Advanced materials and high-technology devices for energy recuperation systems” (2014-2020.4.01.15-0011), NAMUR ”Nanomaterials - research and applications” (3.2.0304.12-0397) and by the Estonian institutional research grant No. IUT20-13.

## ORCID

E. Hark¨ https://orcid.org/0000-0001-5758-8106
E. Lust https://orcid.org/0000-0002-7942-1558

## References

1. Y. Wang, K. S. Chen, J. Mishler, S. C. Cho, and X. C. Adroher, *Appl. Energy*, **88**, 981 (2011).
2. J. Stacy, Y. N. Regmi, B. Leonard, and M. Fan, *Renewable Sustainable Energy Rev.*, **69**, 401 (2017).
3. Z. Chen, D. Higgins, A. Yu, L. Zhang, and J. Zhang, *Energy Environ. Sci.*, **4**, 3167 (2011).
4. C. W. B. Bezerra, L. Zhang, K. Lee, H. Liu, A. L. B. Marques, E. P. Marques, H. Wang, and J. Zhang, *Electrochim. Acta*, **53**, 4937 (2008).
5. G. Wu, K. L. More, C. M. Johnston, and P. Zelenay, *Science*, **332**, 443 (2011).
6. G. Wu. A. Santandreu, W. Kellogg, S. Gupta, O. Ogoke, H. Zhang, H.-L. Wang, and L. Dai, *Nano Energy*, **29**, 83 (2016).
7. J. Du, F. Y. Cheng, S. W. Wang, T. R. Zhang, and J. Chen, *Sci. Rep.*, **4**, 4386 (2014).
8. K. C. Heo, K. S. Nahm, S.-H. Lee, and P. Kim, *J. Ind. Eng. Chem.*, **17**, 304 (2011).
9. R. Kothandaraman, V. Nallathambi, K. Artyushkova, and S. C. Barton, *Appl. Catal., B*, **92**, 209 (2009).
10. R. Jager,¨ P. E. Kasatkin, E. Hark,¨ P. Teppor, T. Romann, R. Harmas,¨ I. Tallo, U. Maeorg,¨ U. Joost, P. Paiste, K. Kirsimae,¨ and E. Lust, *J. Electroanal. Chem.*, **823**, 593 (2018).
11. F. Roncaroli, E. S. D. Molin, F. A. Viva, M. M. Bruno, and E. B. Halac, *Electrochim. Acta*, **174**, 66 (2015).
12. H. T. Chung, D. A. Cullen, D. Higgins, B. T. Sneed, E. F. Holby, K. L. More, and P. Zelenay, *Science*, **357**, 479 (2017).
13. D. Banham, T. Kishimoto, Y. Zhou, T. Sato, K. Bai, J. Ozaki, Y. Imashiro, and S. Ye, *Sci. Adv.*, **4**, (2018).
14. S. Ratso, I. Kruusenberg, A. Sarapuu, M. Kook, P. Rauwel, R. Saar, J. Aruvali,¨ and K. Tammeveski, *Electrochim. Acta*, **218**, 303 (2016).
15. K. Jukk, N. Kongi, K. Tammeveski, R. M. Aran´-Ais, J. Solla-Gullon,´ and J. M. Feliu, *Electrochim. Acta*, **251**, 155 (2017).
16. P. E. Kasatkin, E. Hark,¨ R. Jager,¨ and E. Lust, *ECS Trans.*, **64**(45), 115 (2015).
17. A. Bonakdarpour, M. Lefevre, R. Yang, F. Jaouen, T. Dahn, J.-P. Dodelet, and J. R. Dahn, *Electrochem. Solid-State Lett.*, **11**, B105 (2008).
18. J. Chlistunoff, *J. Phys. Chem. C*, **115**, 6496 (2011).
19. A. Gabe, J. Garcia-Aguilar, A. Berenguer-Murcia, E. Morallon,´ and D. Cazorla-Amoros,´ *Appl. Catal., B*, **217**, 303 (2017).
20. F. Jaouen and J.-P. Dodelet, *Electrochim. Acta*, **52**, 5975 (2007).
21. T. Lopes, A. Kucernak, D. Malko, and E. A. Ticianelli, *ChemElectroChem*, **3**, 1580 (2016).
22. Y. J. Sa, D.-J. Seo, J. Woo, J. T. Lim, J. Y. Cheon, S. Y. Yang, J. M. Lee, D. Kang, T. J. Shin, H. S. Shin, H. Y. Jeong, C. S. Kim, M. G. Kim, T.-Y. Kim, and S. H. Joo, *J. Am. Chem. Soc.*, **138**, 15046 (2016).
23. J. Ozaki, S. Tanifuji, A. Furuichi, and K. Yabutsuka, *Electrochim. Acta*, **55**, 1864 (2010).
24. P. Teppor, R. Jager,¨ E. Hark,¨ U. Joost, I. Tallo, P. Paiste, K. Kirsimae,¨ and E. Lust, *ECS Trans.*, **85**(13), 855 (2018).
25. E. Tee, I. Tallo, H. Kurig, T. Thomberg, A. Janes,¨ and E. Lust, *Electrochim. Acta*, **161**, 364 (2015).
26. P. E. Kasatkin, R. Jager,¨ E. Hark,¨ P. Teppor, I. Tallo, U. Joost, K. Smits, R. Kanarbik, and E. Lust, *Electrochem. Commun.*, **80**, 33 (2017).
27. M. P. Seah, I. S. Gilmore, and S. J. Spencer, *J. Electron Spectrosc. Relat. Phenom.*, **120**, 93 (2001).
28. P. I. Ravikovitch and A. V. Neimark, *Colloids Surf., A*, **187–188**, 11 (2001).
29. Y. Chen, S. Jie, C. Yang, and Z. Liu, *Appl. Surf. Sci.*, **419**, 98 (2017).
30. F. A. Westerhaus, R. V. Jagadeesh, G. Wienhofer,¨ M.-M. Pohl, J. Radnik, A.-E. Surkus, J. Rabeah, K. Junge, H. Junge, M. Nielsen, A. Bruckner,¨ and M. Beller, *Nature Chem.*, **5**, 537 (2013).
31. P. Zhou, L. Jiang, F. Wang, K. Deng, K. Lv, and Z. Zhang, *Sci. Adv.*, **3**, (2017).
32. D. Cabrera-German, G. Gomez-Sosa, and A. Herrera-Gomez, *Surf. Interface Anal.*, **48**, 252 (2016).
33. K. Artyushkova, S. Levendosky, P. Atanassov, and J. Fulghum, *Top. Catal.*, **46**, 263 (2007).
34. D. Guo, R. Shibuya, C. Akiba, S. Saji, T. Kondo, and J. Nakamura, *Science*, **351**, 361 (2016).
35. G. Liu, X. Li, P. Ganesan, and B. N. Popov, *Electrochim. Acta*, **55**, 2853 (2010).
36. S. Kabir, K. Artyushkova, A. Serov, B. Kiefer, and P. Atanassov, *Surf. Interface Anal.*, **48**, 293 (2016).
37. F. Jaouen, S. Marcotte, J.-P. Dodelet, and G. Lindbergh, *J. Phys. Chem. B*, **107**, 1376 (2003).
38. D. D. Do, *Series on Chemical Engineering, vol. 2, Adsorption Analysis: Equilibria and Kinetics*, p. 795 (1998).
39. J. L. Figueiredo, M. F. R. Pereira, M. M. A. Freitas, and J. J. M. Orfao,˜ *Carbon*, **37**, 1379 (1999).
40. S. Li, L. Zhang, H. Liu, M. Pan, L. Zan, and J. Zhang, *Electrochim. Acta*, **55**, 4403 (2010).
41. Y. Zheng, Y. Jiao, Y. Zhu, Q. Cai, A. Vasileff, L. H. Li, Y. Han, Y. Chen, and S.-Z. Qiao, *J. Am. Chem. Soc.*, **139**, 3336 (2017).
42. L. C. P. Perez,´ N. R. Sahraie, J. Melke, P. Elsasser,¨ D. Teschner, X. Huang, R. Kraehnert, R. J. White, S. Enthaler, P. Strasser, and A. Fischer, *Adv. Funct. Mater.*, **28**, 1707551 (2018).
43. J. Perez, E. R. Gonzales, and E. A. Ticianelli, *Electrochim. Acta*, **44**, 1329 (1998).
44. C. Song and J. Zhang, in *PEM Fuel Cell Electrocatalysts and Catalyst Layers: Fundamentals and Applications*, J. Zhang, Editor, p. 91, Springer-Verlag, London (2008).
45. D. Banham, S. Ye, K. Pei, J. Ozaki, T. Kishimoto, and Y. Imashiro, *J. Power Sources*, **285**, 334 (2015).

Institute of Solid State Physics, University of Latvia as the Center of Excellence has received funding from the European Union’s Horizon 2020 Framework Programme H2020-WIDESPREAD-01-2016-2017-TeamingPhase2 under grant agreement No. 739508, project CAMART²